JOURNAL OF BACTERIOLOGY, Mar. 2004, p. 1287–1296 Vol. 186, No. 5
0021-9193/04/$08.00+0 DOI: 10.1128/JB.186.5.1287–1296.2004

Transcriptional Regulation of Genes Encoding Arabinan-Degrading Enzymes in *Bacillus subtilis*

Maria Paiva Raposo,[1]† José Manuel Inácio,[1] Luís Jaime Mota,[1]‡ and Isabel de Sá-Nogueira[1,2]*

Instituto de Tecnologia Química e Biológica, Universidade Nova de Lisboa, 2781-901 Oeiras,[1] and Faculdade de Ciências e Tecnologia, Universidade Nova de Lisboa, Quinta da Torre, 2829-516 Caparica,[2] Portugal

Received 25 August 2003/Accepted 14 November 2003

Bacillus subtilis **produces hemicellulases capable of releasing arabinosyl oligomers and arabinose from plant cell walls. In this work, we characterize the transcriptional regulation of three genes encoding arabinan-degrading enzymes that are clustered with genes encoding enzymes that further catabolize arabinose. The *abfA* gene comprised in the metabolic operon *araABDLMNPQ-abfA* and the *xsa* gene located 23 kb downstream most probably encode α-L-arabinofuranosidases (EC 3.2.1.55). Here, we show that the *abnA* gene, positioned immediately upstream from the metabolic operon, encodes an endo-α-1,5-arabinanase (EC 3.2.1.99). Furthermore, by in vivo RNA studies, we inferred that *abnA* and *xsa* are monocistronic and are transcribed from σ^A-like promoters. Transcriptional fusion analysis revealed that the expression of the three arabinases is induced by arabinose and arabinan and is repressed by glucose. The levels of induction by arabinose and arabinan are higher during early postexponential growth, suggesting a temporal regulation. Moreover, the induction mechanism of these genes is mediated through negative control by the key regulator of arabinose metabolism, AraR. Thus, we analyzed AraR-DNA interactions by in vitro quantitative DNase I footprinting and in vivo analysis of single-base-pair substitutions within the promoter regions of *xsa* and *abnA*. The results indicate that transcriptional repression of the *abfA* and *xsa* genes is achieved by a tightly controlled mechanism but that the regulation of *abnA* is more flexible. We suggest that the expression of genes encoding extracellular degrading enzymes of arabinose-containing polysaccharides, transport systems, and intracellular enzymes involved in further catabolism is regulated by a coordinate mechanism triggered by arabinose via AraR.**

Hemicellulose is the second-most abundant renewable biomass polymer, next to cellulose. This fraction of plant cell walls comprises a complex mixture of polysaccharides that includes xylans, arabinans, galactans, mannans, and glucans. Enzymes responsible for degrading plant cell wall polysaccharides have many agroindustrial applications, such as biobleaching of pulps in the pulp and paper industry, improving digestibility of animal feedstock, processing of flour in the baking industry, and clarifying juices (references 6, 26, and 27, and references therein). Although many hemicellulases have been purified and characterized from both fungi and bacteria, including mesophilic and thermophilic *Bacillus* spp., knowledge concerning regulation at the molecular level of hemicellulolytic genes is scarce (reference 34 and references therein).

The saprophytic endospore-forming gram-positive bacterium *Bacillus subtilis* participates in enzymatic dissolution of plant cell walls in its natural reservoir, the soil. L-Arabinose is distributed in hemicelluloses and is present at high concentrations in arabinoxylans, arabinogalactans, and arabinan. The latter is composed of α-1,5-linked L-arabinofuranosyl units, some of which are replaced with α-1,3- and α-1,2-linked chains of L-arabinofuranosyl residues (2). The two major enzymes that hydrolyze arabinan are α-L-arabinofuranosidases (AFs) (EC 3.2.1.55) and endo-α-1,5-arabinanases (ABNs) (EC 3.2.1.99). AFs remove arabinose side chains, allowing ABNs to attack the glycosidic bonds of the arabinan backbone and releasing a mixture of arabinooligosaccharides and L-arabinose (9). *B. subtilis* synthesizes at least three enzymes, an ABN and two AFs, capable of releasing arabinosyl oligomers and L-arabinose from plant cell walls (12, 13, 28, 39).

Previous work by our group characterized the genes involved in the utilization of L-arabinose that belong to the *araABDLMNPQ-abfA* operon (32) and the divergently arranged *araE* and *araR* genes (31, 33), located in distinct regions of the *B. subtilis* chromosome. The first three genes of the L-arabinose metabolic operon, *araA*, *araB*, and *araD*, encode the enzymes required for the intracellular conversion of L-arabinose into D-xylulose 5-phosphate, which is further catabolized through the pentose phosphate pathway (30). The product of the *araE* gene is a permease, the main transporter of L-arabinose into the cell (33). The *araR* gene encodes the regulatory protein of L-arabinose metabolism in *B. subtilis*, negatively controlling the expression from the L-arabinose-inducible promoters of the *ara* genes (22, 23). Additionally, the *ara* regulon is subjected to carbon catabolite repression by glucose and glycerol (11). The last gene of the L-arabinose metabolic operon, *abfA*, and the *xsa* gene located 23 kb downstream from the operon (32, 40) (Fig. 1) most probably encode AFs belonging to the glycosyl hydrolase (GH) family G51 (see the Carbohydrate-Active Enzymes website [http://afmb.cnrs-mrs.fr/~cazy/CAZY]). The gene *abnA*, located immediately upstream from the metabolic operon (32, 40) (Fig. 1), most likely en-

* Corresponding author. Mailing address: Instituto de Tecnologia Química e Biológica, Universidade Nova de Lisboa, Avenida da República, Apartado 127, 2781-901 Oeiras, Portugal. Phone: (351) 21-4469524. Fax: (351) 21-4411277. E-mail: sanoguei@itqb.unl.pt.

† Present address: Department of Biochemistry and Molecular Biology, University of Miami, School of Medicine, Miami, FL 33136.

‡ Present address: Biozentrum der Universität Basel, 50-70 CH-Basel, Switzerland.

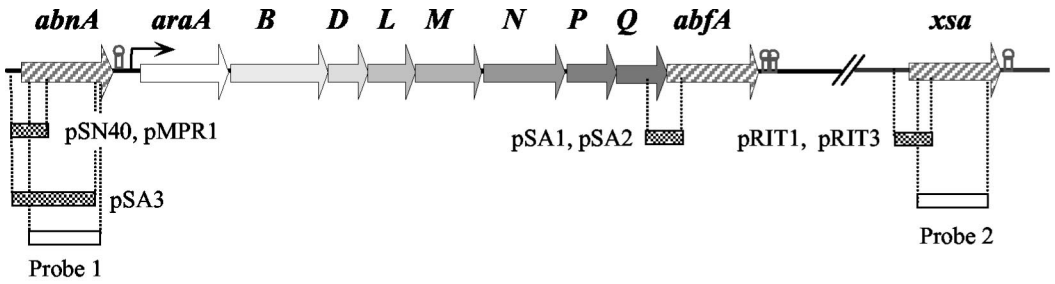

FIG. 1. Localization of the *abnA*, *abfA*, and *xsa* genes on the *B. subtilis* chromosome. The three genes are represented by striped arrows pointing in the direction of transcription. *abfA* belongs to the *araABDLMNPQ-abfA* metabolic operon, *abnA* is located immediately upstream, and the *xsa* gene is positioned 23 kb downstream of the metabolic operon. Hairpin structures indicate potential terminators. The dotted boxes below the physical map represent the extension of the inserts fused to the *lacZ* gene in the indicated plasmids, and the open boxes represent the fragments used as probes for Northern analysis of the *abnA* (probe 1) and *xsa* (probe 2) transcripts. Plasmids pMPR1, pSA1, and pRIT3 were integrated into the host chromosome by means of a single-crossover (Campbell-type) recombinational event that occurred in the region of homology of the resulting strains (Table 1). Linearized DNA from plasmids pSN40, pSA3, pSA2, and pRIT1 was used to transform *B. subtilis* strains (Table 1), and the fusions were integrated into the chromosome via double recombination with the back and front sequences of the *amyE* gene.

codes an ABN grouped in the GH43 family (http://afmb.cnrs-mrs.fr/~cazy/CAZY).

Our work focuses on the regulation of expression of the *abfA*, *xsa*, and *abnA* genes. Additionally, functional analysis of *abnA* revealed that this gene encodes an ABN. In vivo RNA studies demonstrated the monocistronic nature of *xsa* and *abnA* and allowed us to characterize their promoter regions. We show that the expression of the *abfA*, *xsa*, and *abnA* genes is positively controlled at the transcriptional level by arabinose and arabinan, repressed by glucose, and most likely subjected to temporal regulation. Moreover, in vivo and in vitro studies indicate that the transcription factor AraR plays a major role in the control of the expression of the arabinan-degrading genes. It is hypothesized that coordinate expression of genes involved in the degradation of arabinose-containing polysaccharides is triggered by arabinose and mediated by AraR.

MATERIALS AND METHODS

Bacterial strains and growth conditions. The *B. subtilis* strains used in this study are listed in Table 1. *Escherichia coli* DH5α (Gibco BRL) was used for routine molecular cloning work and was grown on Luria-Bertani (LB) medium (20). Ampicillin (75 μg ml^{-1}), X-Gal (5-bromo-4-chloro-3-indolyl-β-D-galactopyranoside; 40 μg ml^{-1}), or IPTG (isopropyl-β-D-thiogalactopyranoside; 1 mM) was added as appropriate. The *B. subtilis* strains were grown on LB medium (20) or C minimal medium (24), and chloramphenicol (5 μg ml^{-1}) or kanamycin (10 μg ml^{-1}) was added as appropriate. Solid medium was made with LB or C minimal medium containing 1.6% (wt/vol) Bacto Agar (Difco). The *abnA* phenotype was tested in C minimal medium (24) plates supplemented with 0.4% (wt/vol) debranched arabinan (Megazyme). The *amyE* phenotype was tested by plating strains on tryptose blood agar base medium (Difco) containing 1% (wt/vol) potato starch, and after overnight incubation, the plates were flooded with a solution of 0.5% (wt/vol) I_2 and 5.0% (wt/vol) KI for the detection of starch hydrolysis. For the β-galactosidase assays and RNA preparation, the *B. subtilis* strains were grown in liquid C minimal medium supplemented with 1% (wt/vol) casein hydrolysate. When necessary, 0.4% (wt/vol) L-arabinose, 0.4% (wt/vol) arabinan (sugar beet; Megazyme), and 0.4% (wt/vol) glucose were added to the cultures. The transformation of *E. coli* and *B. subtilis* strains was performed as previously described (23).

DNA manipulations and sequencing. DNA manipulations were carried out as described by Sambrook et al. (29). Restriction enzymes were purchased from MBI Fermentas and New England Biolabs and used according to the manufacturer's instructions. DNA was eluted from agarose gels with a GENECLEANII kit (Bio101). DNA sequencing was performed with a Sequenase version 2.0 kit (USB) or an ABI PRIS BigDye terminator ready reaction cycle sequencing kit (Applied Biosystems). PCR amplifications were done by using high-fidelity native *Pfu* DNA polymerase (Stratagene), and the products were purified by using a QIAquick PCR purification kit (QIAGEN).

TABLE 1. *B. subtilis* strains used in this study

Strain	Genotype or description	Source or reference[a]
168T$^+$	Prototroph	F. E. Young
IQB215	Δ*araR*::Km	31
IQB405	*amyE*::[*xsa′-lacZ cat*]	pRIT1 → 168T^{+b}
IQB406	*amyE*::[*xsa′-lacZ cat*] Δ*araR*::Km	pRIT1 → IQB215[b]
IQB407	*xsa*::pRIT3[*xsa′-lacZ cat*]	pRIT3 → 168T$^+$
IQB410	*amyE*::[*abnA′-lacZ cat*]	pSN40 → 168T^{+b}
IQB411	*amyE*::[*abnA′-lacZ cat*] Δ*araR*::Km	pSN40 → IQB215[b]
IQB412	*abnA*::pMPR1[*abnA′-lacZ cat*]	pMPR1 → 168T$^+$
IQB413	Δ*abnA*::Km	pMPR4 → 168T^{+b}
IQB448	*amyE*::[*abnA′-lacZ cat*]	pSA3 → 168T^{+b}
IQB449	*amyE*::[*abnA′-lacZ cat*] Δ*araR*::Km	pSA3 → IQB215[b]
IQB450	*abfA*::pSA1[*abfA′-lacZ cat*]	pSA1 → 168T$^+$
IQB451	*amyE*::[*abfA′-lacZ cat*]	pSA2 → 168T^{+b}
IQB453	*abfA*::pSA1[*abfA′-lacZ cat*] Δ*araR*::Km	pSA1 → IQB215
IQB464	*amyE*::[*abnA′*(−38 G → T)-*lacZ cat*]	pZI15 → 168T^{+b}
IQB465	*amyE*::[*xsa′*(−27 G → T)-*lacZ cat*]	pZI19 → 168T^{+b}

[a] The arrows indicate transformation and point from donor DNA to the recipient strain.
[b] Transformation was carried out with linearized plasmid DNA.

TABLE 2. *B. subtilis* oligonucleotides and sequences used in this study

Primer	Sequences (5′ → 3′)[a]	Complementary sequence
ARA1	$^{-39}$TAAGGGTAACTATTGCCG^{-22}	pSN32
ARA32	$^{+124}$GAATTCAGGATCCTTTGTCTGAAGC^{+100}	*araA*
ARA72	$^{+35}$AGTGTATCAACAAGCTGG^{+17}	pSN32
ARA85	$^{-171}$GTGATGATTATGAATTCGCGG^{-157}	*abnA*
ARA86	$^{+160}$CACTCGAAAAGTGTAAGAAGCG^{+139}	*abnA*
ARA87	$^{-207}$AAAATAGCGGATTACGGCATCG^{-186}	*xsa*
ARA88	$^{+189}$CCTAAATGCTCAGCAAAATGACC^{+167}	*xsa*
ARA89	$^{+936}$ATCCAAAATGGTGCCTCCG^{+918}	*abnA*
ARA90	$^{+124}$GAATCACTGCTTGATGTTCAGACATGCC^{+97}	*xsa*
ARA91	$^{+1509}$GTATTGTCTGCAGGATTCCGG^{+1489}	*xsa*
ARA92	$^{+879}$GCCTGTAATGCTTTTAGATCTTCC^{+856}	*abnA*
ARA113	$^{-44}$GAAAATGTCGTTGACATTTACGAACATATATAATATGG^{-7}	*xsa*
ARA114	$^{-7}$CCATATTATATATGTTCGTAAATGTCAACGACATTTTC^{-44}	*xsa*
ARA129	$^{-52}$GATTCTATTTTTTTTTCTGTACAAATTACAGC^{-21}	*abnA*
ARA130	$^{-21}$GCTGTAATTTGTACAGAAAAAAAAATAGAATC^{-52}	*abnA*

[a] The numbers in the primers sequences refer to the positions of the sequence in *abnA* or *xsa* relative to the transcription start point of each gene or to the positions in pSN32 relative to the *Eco*RI site (+1) in the multiple cloning site. The following restriction sites are underlined in the oligonucleotides sequences: *Eco*RI, GAATTC; *Pst*I, CTGCAG; *Bgl*II, AGATCT; *Bam*HI, GGATCC.

Construction of plasmids and strains. The *xsa* and *abnA* promoter regions were amplified by PCR of chromosomal DNA of wild-type strain *B. subtilis* 168T$^+$ with oligonucleotides ARA87 and ARA88 and oligonucleotides ARA85 and ARA86 (Table 2), respectively. Plasmid pRIT1 was obtained by cloning a 281-bp *Eco*RI-*Eco*RV DNA fragment, obtained from the PCR product bearing the *xsa* promoter region, into pSN32 (22) digested with *Eco*RI and *Sma*I. An insertion of the same fragment into pJM783 (25) restricted with *Eco*RI and *Sma*I yielded plasmid pRIT3. To construct plasmid pSN40, the PCR product bearing the *abnA* promoter region was digested with *Eco*RI and *Xmn*I, and the resulting 292-bp product was inserted into pSN32 restricted with *Eco*RI and *Sma*I. Plasmid pMPR1 was obtained by ligation of a 300-bp *Eco*RI-*Bam*HI DNA fragment from pSN40, containing the *abnA* promoter region, to the pJM783 *Eco*RI-*Bam*HI sites. A PCR product bearing the *abnA* promoter region, amplified from chromosomal DNA of wild-type strain *B. subtilis* 168T$^+$ with oligonucleotides ARA85 and ARA89 (Tables 1 and 2) and digested with *Eco*RI-*Sac*I, was inserted into the pBluescript II SK(+) (Stratagene) *Eco*RI-*Sac*I sites, to yield pMPR2. To construct plasmid pSA1, a 687-bp DNA fragment from the *araABDLMNPQ-abfA* operon carrying the 3′ end of the *araQ* gene and the 5′ end of the *abfA* gene (Fig. 1), obtained by *Eco*RI-*Hin*cII digestion of plasmid pTN13 (32), was ligated to the pJM783 (25) *Eco*RI-*Sma*I sites. The same DNA fragment inserted into pSN32 restricted with *Eco*RI and *Sma*I yielded pSA2. Plasmid pSA3 was constructed by insertion of a 1,024-bp PCR product, amplified from chromosomal DNA of wild-type strain *B. subtilis* 168T$^+$ with oligonucleotides ARA85 and ARA92 (Tables 1 and 2) and digested with *Eco*RI-*Bgl*II, into the pSN32 *Eco*RI-*Bam*HI sites. The sequences of all the inserts obtained by PCR were confirmed by DNA sequencing.

To construct pZI15, which carries a single-base-pair substitution in the AraR binding site OR_{B1} (−38 G→T), plasmid pZI13, a pBluescript II SK(+) (Stratagene) derivative containing a 302-bp *Eco*RI-*Bam*HI insert from pSN40, was used as the target DNA for site-directed mutagenesis with the QuikChange kit (Stratagene) and the overlapping oligonucleotides ARA129 and ARA130 (Table 2). An *Eco*RI-*Bam*HI DNA fragment from the resulting plasmid, pZI14, was subcloned into those sites of pSN32 to yield pZI15. To perform a single-nucleotide substitution in the AraR binding site OR_{X2} (−27 G→T), plasmid pZI17, a pBluescript II SK(+) (Stratagene) derivative containing a 291-bp *Eco*RI-*Bam*HI insert from pRIT1, was used as target DNA for site-directed mutagenesis and for the overlapping primers ARA113 and ARA114 (Table 2), as described above. An *Eco*RI-*Bam*HI DNA fragment from the resulting plasmid, pZI18, was ligated to the pSN32 *Eco*RI-*Bam*HI sites to obtain pZI19. The single point mutations were confirmed by DNA sequencing.

Linearized plasmid DNA from pSN40, pRIT1, pSA2, pSA3, pZI15, and pZI19 (Fig. 1), carrying the different promoter-*lacZ* transcriptional fusions, was used to transform *B. subtilis* strains (Table 1), and the fusions were integrated into the chromosome via double recombination with the back and front sequences of the *amyE* gene. This event led to the disruption of the *amyE* locus and was confirmed as described above. Plasmids pRIT3, pMPR1, and pSA1 (Fig. 1) were integrated into the host chromosome by means of a single-crossover (Campbell-type) recombinational event that occurred in the region of homology (Table 1).

A PCR product containing the entire *abnA* gene, amplified from chromosomal DNA of wild-type strain *B. subtilis* 168T$^+$ with oligonucleotides ARA32 and ARA85 (Tables 1 and 2), was digested with *Dde*I-*Bam*HI, and this fragment bearing the 3′ end of *abnA* was inserted in the pSN32 *Sma*I-*Bam*HI sites to yield pSN41. Plasmid pSN42 was the result of the insertion of a 535-bp *Eco*RI-*Bam*HI DNA fragment from pSN41 into the pBluescript II SK(+) (Stratagene) *Eco*RI-*Bam*HI sites. To construct plasmid pMPR3, a 1.5-kb *Sph*I-*Sma*I DNA fragment from pAH248 (31) containing a kanamycin resistance (Km^r) gene was inserted into the pSN42 *Sph*I-*Sma*I site. By subcloning a 1,626-bp *Sal*I DNA fragment from pSN40 (see above) at the unique *Sal*I site of pMPR3, pMPR4 was obtained. This plasmid was used, after linearization, to delete the *abnA* gene from the wild-type *B. subtilis* 168T$^+$ chromosome.

β-Galactosidase assays. Strains of *B. subtilis* harboring the transcriptional *lacZ* fusions were grown as described above. Samples of cell culture were collected 2 h (exponential growth phase) and 4 h (late exponential growth phase) after induction, and the level of β-galactosidase activity was determined as previously described (32). The ratio of β-galactosidase activity from cultures grown in the presence or absence of an inducer (arabinose or arabinan) was taken as a measure of AraR repression in each strain analyzed (regulation factor). The ratio of β-galactosidase activity from cultures grown in the presence or absence of glucose was taken as a measure of glucose repression (glucose repression factor).

RNA preparation, Northern blot analysis, and primer extension analysis. *B. subtilis* strains were grown as described above, and cells were harvested 2 h after induction. Total RNA was prepared by using an RNeasy kit (QIAGEN) according to the manufacturer's instructions. For Northern blot analysis, 10 μg of total RNA was run in a 1.2% (wt/vol) agarose formaldehyde denaturing gel and transferred to positively charged Hybond-N$^+$ (Amersham) nylon membranes according to standard procedures (29). A size determination was done by using an RNA ladder (9 to 0.5 kb [New England Biolabs] or 6 to 0.2 kb [MBI Fermentas]). A DNA fragment of 763 bp used as an *abnA* probe was obtained by PCR amplification of chromosomal DNA with primers ARA85 and ARA89 followed by *Pst*I digestion. PCR amplification with chromosomal DNA as a template and primers ARA87 and ARA91 (Table 2) yielded a DNA fragment that, after digestion with *Bcl*I, resulted in a 1.4-kb *xsa* DNA probe. The DNA probes were labeled with a Megaprime DNA labeling system (Amersham) and [α-^{32}P]dCTP (3,000 Ci/mmol; Amersham).

Primer extension analysis was performed essentially as described by Sambrook et al. (29). Primer ARA86, complementary to the *abnA* sequence (Table 2), and primer ARA90, complementary to the *xsa* sequence (Table 2), were end labeled with [γ-^{32}P]ATP (3,000 Ci/mmol) by using T4 polynucleotide kinase (NEB). A total of 2.5 ρmol of each labeled primer was mixed with 50 to 100 μg of RNA in separate experiments, denatured by heating to 85°C for 10 min, and annealed by incubation at 45°C overnight. The extension reaction was conducted for 2 h at 37°C by using 50 U of avian Moloney murine leukemia virus reverse transcriptase (RevertAid; MBI Fermentas). Analysis of the extended products was carried out on 6% (wt/vol) polyacrylamide urea gels.

DNase I footprinting. The target DNA fragments from the *xsa* and *abnA* promoters were obtained by PCR amplification with oligonucleotides ARA1 and

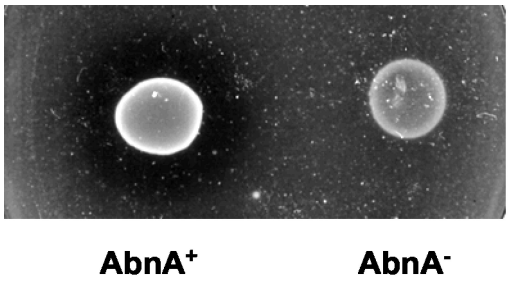

FIG. 2. Functional analysis of the *abnA* gene. The *B. subtilis* wild-type strain 168T$^+$ (AbnA$^+$) and the *abnA*-null mutant strain IQB413 (AbnA$^-$) were grown on C minimal medium plates (see Materials and Methods) supplemented with 0.4% (wt/vol) debranched arabinan for 48 h at 37°C.

ARA72 (Table 2) using pRIT1 and pSN40 (see above) as templates and yielding 339- and 350-bp DNA fragments, respectively. The labeling of the fragments and the DNase I footprinting experiments were performed by using purified native AraR as previously described by Mota et al. (22). The apparent dissociation constant (K_{app}) for the different operators was determined as the total concentration of AraR required for half-maximal site protection.

RESULTS

The *abfA* and *xsa* genes and functional analysis of the *abnA* gene. The *abfA* and the *xsa* genes most probably encode AFs (EC 3.2.1.55). The amino acid sequence of AbfA displays a high level of identity (71%) to characterized AbfA from *Geobacillus stearothermophilus* T-6 (8), and AF activity was reported for the *B. subtilis abfA* gene product (40). Xsa is highly homologous to characterized AFs from *Thermobacillus xylanilyticus* AbfD3 (64% identity) (3), *Clostridium cellulovorans* ArfA (60% identity) (15), and *Clostridium stercorarium* ArfB (56% identity) (42). Based on primary amino acid sequence analysis, the *abnA* gene most likely encodes an ABN (EC 3.2.1.99), with 52% identity to a characterized thermostable ABN from *Bacillus thermodinitrificans* (36) and 38% identity to ArbA from *Cellvibrio japonicus* (19). Previously, Sakamoto et al. (28) reported the cloning of the gene *ppc* from *B. subtilis* strain IFO 3134 that encodes an ABN displaying 94% identity to the product of the *abnA* gene from *B. subtilis* 168T$^+$. However, it is unclear whether the arabinan-degrading activity measured in that strain reflects the expression of the *ppc* gene (28). To characterize the function of the *abnA* gene, we constructed an insertion-deletion mutation in the *abnA* region (see Materials and Methods). The *abnA*-null mutant strain (IQB413) (Table 1) was able to grow on minimal medium plates supplemented with debranched arabinan (see Materials and Methods), although more slowly than the wild-type strain. However, the clear halo of hydrolysis observed for the wild-type strain was absent in the mutant (Fig. 2), indicating that the product of the *abnA* gene is an ABN.

***abnA* and *xsa* transcript analysis.** Previous work showed that the *abfA* gene encodes a 500-amino-acid polypeptide and belongs to the *araABDLMNPQ-abfA* operon, a polycistronic transcriptional unit responsive to arabinose (32) (Fig. 1). The *abnA* and *xsa* genes encode 323- and 495-amino-acid polypeptides, respectively, and both potential open reading frame terminators were found downstream (32, 40) (Fig. 1). To study transcription of the *abnA* and *xsa* genes, total RNA isolated from the wild-type strain grown for 2 h in the absence or presence of arabinose and arabinan (potential inducers) was annealed separately to DNA probes for *abnA* and *xsa*. Arabinose-inducible *abnA*- and *xsa*-specific transcripts of about 0.9 and 1.6 kb, respectively, were detected (Fig. 3). Weaker hybridization signals of the same size were also visible with RNA from cells grown in the presence of arabinan. No hybridization signals were detected in the absence of sugars, suggesting that both arabinose and arabinan might function as inducers. The extent of both *abnA* and *xsa* mRNA signals closely matched the expected sizes (1 and 1.6 kb, respectively) and confirm their

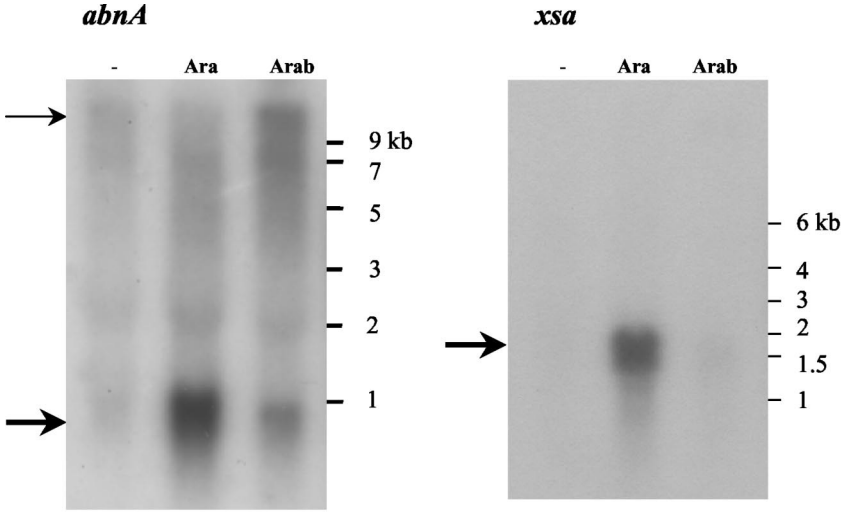

FIG. 3. Northern blot analysis of the *abnA*- and *xsa*-specific transcripts. Ten micrograms of total RNA extracted from the wild-type strain grown in the absence of sugar (−), in the presence of arabinose (Ara), or in the presence of arabinan (Arab) was run in a 1.2% (wt/vol) agarose formaldehyde denaturing gel (see Materials and Methods). The RNA ladder used as molecular size markers is indicated to the right of each gel. The *abnA*-specific (left) and *xsa*-specific (right) transcripts detected with DNA probe fragments *abnA* (767 bp) and *xsa* (1,420 bp) are indicated by heavy arrows. The additional weak high-molecular-weight RNA signal visible with the *abnA* DNA probe (left) is indicated by a light arrow.

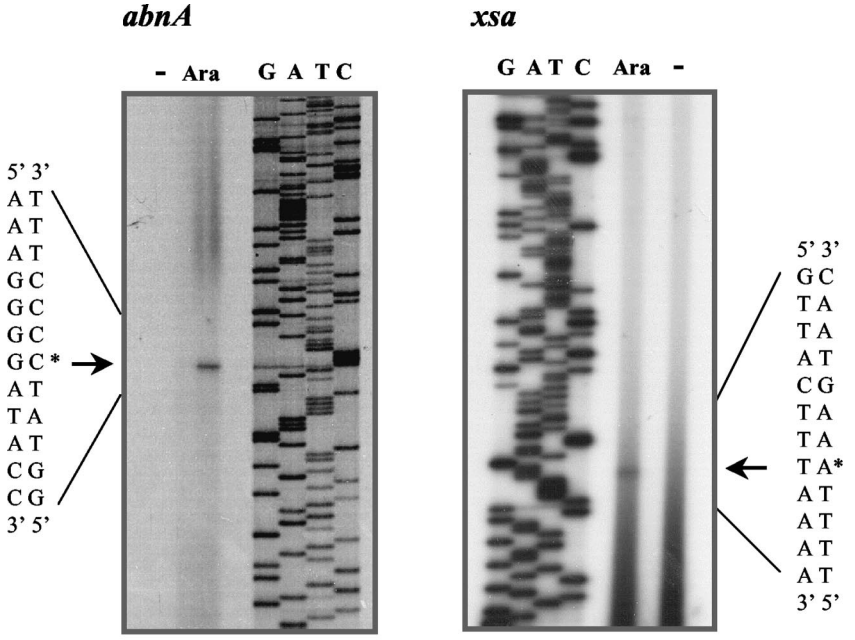

FIG. 4. Mapping of the transcriptional start site of the *abnA* and *xsa* genes. Radiolabeled oligonucleotides ARA86 and ARA90 (Table 2), complementary to the *abnA* and *xsa* sequences, respectively, were hybridized and used to direct cDNA synthesis from total *B. subtilis* 168T$^+$ RNA isolated from exponentially growing cells in the absence (−) or presence (Ara) of arabinose (see Materials and Methods). After extension, the products were analyzed by gel electrophoresis together with a set of dideoxynucleotide chain termination sequencing reactions by using the same primers and plasmids pMPR2 and pRIT3, respectively, as templates. Arrows and asterisks indicate the positions of the *abnA*- and *xsa*-specific primer extension products and the deduced start site of transcription, a G residue in the *abnA* sequence (left) and a T residue in the *xsa* sequence (right).

monocistronic nature. However, when arabinan was used as an inducer, a weak high-molecular-weight RNA signal was visible with the *abnA* DNA probe. One possibility for this finding is that this weak message corresponds to cotranscription with upstream genes and/or the downstream *araABDLMNPQ-abfA* operon.

Expression of *abnA* and *xsa* is driven from σ^A-like promoters. Primer extension analysis of total RNA isolated from cells grown in the presence of arabinose showed that the 5′ end of the *abnA* message corresponds to a G residue 117 bp upstream from the initiation TTG codon (Fig. 4 and 5A). Centered at −35 and −10 bp upstream from the *abnA* transcription start site are two sequences, TGTACA and TACAAT, respectively (Fig. 5A), that are similar to the consensus sequences for recognition by *B. subtilis* σ^A-containing RNA polymerase (TT GACA-17bp-TATAAT) (10, 21). By using the same technique, the apparent transcriptional start point of *xsa* was assigned to a T nucleotide 100 bp upstream from the initiation ATG codon (Fig. 4 and 5B). The potential −35 and −10 regions (TTGA CA-17bp-TATGGT) (Fig. 5B) closely match the σ^A consensus (see above). No *abnA*- or *xsa*-specific extension products were seen with RNA extracted from cells grown in the absence of sugar, results parallel to those observed by Northern blot analysis.

***abnA*, *xsa*, and *abfA* transcription is responsive to arabinose and arabinan and is repressed by glucose.** To study the functionality of the *abnA* and *xsa* promoters, they were fused to the *lacZ* gene of *E. coli* and integrated at the *amyE* locus of the *B. subtilis* wild-type chromosome (strains IQB410 and IQB405, respectively) (Fig. 1 and Table 1). Since transcription of the *abfA* gene is driven from a σ^A-like promoter located upstream from the *araA* gene of the metabolic operon, expression of *abfA* was analyzed by the construction of a transcriptional *lacZ* fusion at the *abfA* locus (strain IQB450) (Fig. 1 and Table 1). The same DNA fragment, harboring the 3′ end of the *araQ* gene and the 5′ end of the *abfA* gene, was also fused to *lacZ* in a different vector and integrated at the *amyE* locus of the *B. subtilis* wild-type chromosome (strain IQB451) (Fig. 1 and Table 1). As expected, this strain did not show promoter activity in the experiments described below (data not shown). The levels of accumulated β-galactosidase activity of the strains bearing the various transcriptional fusions were examined in the absence of sugars and in the presence of arabinose, arabinan, and arabinose plus glucose. Samples were collected 2 and 4 h after induction (t_2 and t_4, respectively), which corresponds to the exponential growth phase and early postexponential phase, respectively. In the presence of arabinose, expression from the *abfA′-lacZ*, *xsa′-lacZ*, and *abnA′-lacZ* fusions (strains IQB450, IQB405, and IQB410) (Table 3) increased during exponential growth about 96-, 24-, and 3-fold, respectively, and a small increment in expression was observed at early postexponential phase (t_4) (Table 3). The presence of arabinan also stimulated expression from the same *abfA′-lacZ*, *xsa′-lacZ*, and *abnA′-lacZ* fusions, about five-, three-, and fivefold, respectively (t_2) (Table 3). However, these lower-level responses, compared to those observed in the presence of arabinose,

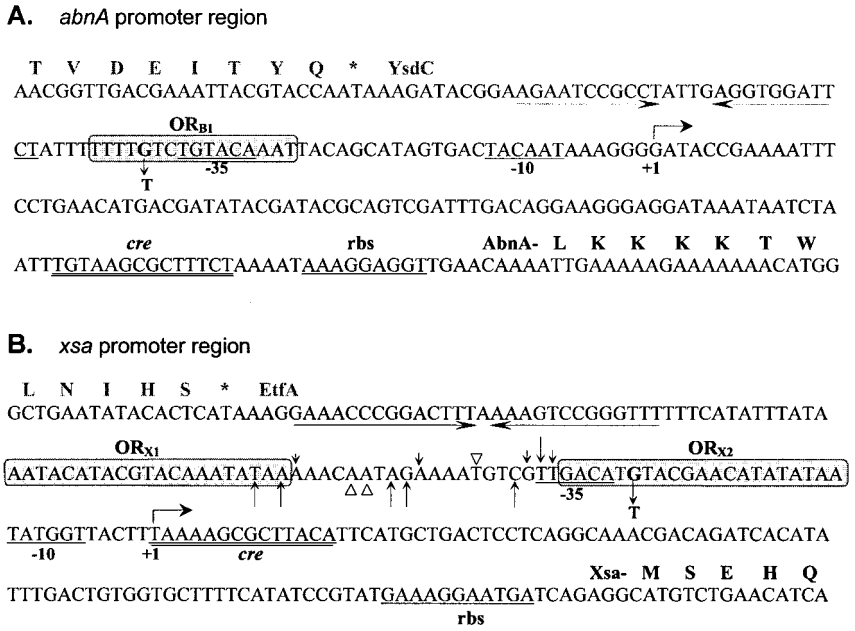

FIG. 5. Promoter regions of the *abnA* and *xsa* genes. The nucleotide sequences of the *abnA* (A) and *xsa* (B) nontranscribed strands are shown in the 5′-to-3′ direction. The transcription start site (+1) defined by primer extension analysis and the −35 and −10 regions of each promoter are indicated below the nucleotide sequence. The putative ribosome binding sites (rbs) are represented, and the potential catabolic repression-associated sequences (CRE) are double underlined. (A) The predicted primary structure of AbnA and the polypeptide encoded by *ysdC* (the upstream gene) is given in single-letter code above the nucleotide sequence. A putative terminator sequence of *ysdC* is represented by convergent arrows. The AraR binding site, OR_{B1}, deduced by similarity and confirmed by site-directed mutagenesis, is represent by a grey box. A single nucleotide change introduced in OR_{B1} at position −38 (G→T) is indicated. (B) The predicted primary structure of Xsa and the polypeptide encoded by *etfA* (the upstream gene) is given in single-letter code above the nucleotide sequence. A putative terminator sequence of *etfA* is represented by convergent arrows. AraR binding regions detected in DNase I footprinting experiments, OR_{X1} and OR_{X2}, are shown in grey boxes. The sites of enhanced (black arrows) and diminished (open triangles) DNase I cleavage outside of the protected regions detected in the noncoding strand are shown above the sequence and in the coding strand below the sequence. The size of the arrow reflects the intensity of enhanced cleavage by DNase I. A single-base-pair substitution introduced in OR_{X2} at position −27 (G→T) is indicated.

increased more dramatically at the end of the exponential growth phase (t_4) (Table 3). These results confirm the Northern blot analysis indicating that both arabinose and arabinan function as inducers of the *abnA*, *xsa*, and *abfA* genes. The possibility that other regulatory regions upstream from the DNA fragments used to construct the *xsa′-lacZ* and *abnA′-lacZ* fusions integrated at the *amyE* locus might influence expression from *xsa* and *abnA* was examined. We constructed transcriptional *lacZ* fusions at the *xsa* and *abnA* loci (strains IQB407 and IQB412) (Table 1), and the regulation factor calculated for these strains was similar to that observed for strains IQB405 and IQB410, respectively (data not shown).

The addition of glucose caused a 21.8-fold repression of the *abfA′-lacZ* fusion expression, a 19.3-fold repression of *xsa′-lacZ* expression, and a 6.5-fold repression of *abnA′-lacZ* expression (t_2) (Table 3). No significant differences in the levels of glucose repression were observed during early postexponential phase (t_4) (Table 3). Previously, it has been shown that glucose repression of the *araABDLMNPQ-abfA* metabolic operon is mainly regulated by CcpA via binding to two catabolite responsive elements (CREs), one located between the promoter region of the operon and the *araA* gene and one located 2 kb downstream within the *araB* gene (11). Mutagenesis studies of *B. subtilis* revealed the CRE consensus sequence TGWAARCGYTWNCW (W = A or T, R = A or G, Y = C or T, N = any base) (14, 18, 38, 41). Based on sequence homology studies, potential CRE sequences were detected in the promoter region of the *abnA* and *xsa* genes. The CRE for *abnA* is positioned between the promoter and the TTG initiation codon ($^{+79}$TGTAAGCGCTTTCT^{+92}) (Fig. 5A), and the CRE for *xsa* overlaps the transcription start site of the gene ($^{+1}$TAAAAGCGCTTACA^{+14}) (Fig. 5B).

AraR plays a major role in transcriptional control of *abnA*, *xsa*, and *abfA*. In previous work, a search of the *B. subtilis* database was done (SubtiList) for sequences similar to the AraR consensus operator (ATTTGTACGTACAAAT) (22), the key regulator of arabinose utilization. Among the potential AraR binding sites detected, two were located in the promoter region of the *xsa* and *abnA* genes (22). Thus, we investigated the expression from the *abfA′-lacZ*, *xsA′-lacZ*, and *abnA′-lacZ* fusions in an *araR*-null mutant background. The levels of accumulated β-galactosidase activity of the resulting strains (IQB453, IQB406, and IQB411, respectively) were examined as described above, and the results are shown in Table 3. The degree of AraR repression (regulation factor) was determined indirectly by the ratio of the values obtained in induced and noninduced cultures. Disruption of the *araR* gene led to a total derepression of the expression from the *abfA′-lacZ*, *xsA′-lacZ*, and *abnA′-lacZ* fusions (strains IQB453, IQB406, and IQB411, respectively) in comparison to that from the wild type. These results suggest that AraR plays a major role in the transcriptional control of the *abnA*, *xsa*, and *abfA* genes. Interestingly,

TABLE 3. Expression from *abfA'-lacZ*, *xsa'-lacZ*, and *abnA'-lacZ* fusions in a wild-type and *araR*-null mutant background[a]

Promoter fusion and strain[b]	Time	β-Galactosidase activity (Miller units)[c]				Regulation/repression factor[d]		
		−Ara	+Ara	+Arab	+Ara +Glc	Ara	Arab	Glc
abfA'-lacZ								
IQB450 (WT)	t_2	3.2 ± 0.7	303.9 ± 28.9	16.8 ± 2.6	13.0 ± 2.3	96.4	5.3	21.8
	t_4	3.2 ± 0.4	490.4 ± 10.1	88.6 ± 6.3	27.8 ± 4.5	153.0	27.6	17.6
IQB453 (AraR$^-$)	t_2	1,363.5 ± 17.4	750.5 ± 125.1	660.1 ± 31.2	ND[e]	0.6	0.5	ND
	t_4	1,957.6 ± 111.0	485.3 ± 62.6	766.1 ± 55.0	ND	0.3	0.4	ND
xsa'-lacZ								
IQB405 (WT)	t_2	7.5 ± 0.2	177.3 ± 3.9	21.8 ± 0.7	9.2 ± 0.5	23.7	2.9	19.3
	t_4	9.0 ± 0.8	287.4 ± 38.6	245.8 ± 23.2	17.2 ± 1.6	31.9	27.2	16.7
IQB406 (AraR$^-$)	t_2	564.0 ± 57.6	503.8 ± 13.4	397.4 ± 4.9	ND	0.8	0.7	ND
	t_4	561.7 ± 74.4	296.2 ± 39.3	679.1 ± 46.7	ND	0.5	1.2	ND
abnA'-lacZ								
IQB410 (WT)	t_2	3.2 ± 0.7	10.0 ± 0.8	15.2 ± 2.1	1.6 ± 0.3	3.1	4.7	6.5
	t_4	3.0 ± 0.4	11.0 ± 0.4	25.7 ± 5.2	1.7 ± 0.0	3.7	8.6	7.5
IQB411 (AraR$^-$)	t_2	31.3 ± 2.0	35.2 ± 0.4	25.9 ± 0.1	ND	1.1	0.8	ND
	t_4	39.6 ± 4.2	25.8 ± 2.4	42.8 ± 1.7	ND	0.7	1.1	ND
IQB448 (WT)	t_2	2.4 ± 0.6	13.2 ± 0.9	17.3 ± 2.7	1.8 ± 0.2	5.6	7.2	7.2
	t_4	1.8 ± 0.2	13.6 ± 1.9	31.5 ± 5.2	2.0 ± 0.3	7.4	17.1	6.8
IQB449 (AraR$^-$)	t_2	58.8 ± 7.5	53.7 ± 4.1	36.8 ± 4.7	ND	0.9	0.6	ND
	t_4	59.1 ± 3.1	67.5 ± 16.5	46.7 ± 7.6	ND	1.1	0.8	ND

[a] The strains containing different promoter-*lacZ* fusions were grown on C minimal medium supplemented with casein hydrolysate in the absence of sugar (−Ara), in the presence of arabinose (+Ara), in the presence of arabinan (+Arab), and in the presence of arabinose plus glucose (+Ara +Glc). Samples were analyzed 2 h (t_2) and 4 h (t_4) after the addition of sugars.

[b] WT, wild type.

[c] The levels of accumulated β-galactosidase activity represent the average of results from three independent experiments with wild-type strains and two independent experiments with AraR$^-$ strains.

[d] The regulation factor, was calculated as the ratio of the level of expression (in Miller units) obtained in the presence of arabinose (Ara) or arabinan (Arab) to the value determined in the absence of sugar (−Ara), was taken as a measure of AraR repression. Glucose repression (Glc) was calculated as the ratio of the level of expression (in Miller units) obtained in the presence of arabinose to the value determined in the presence of glucose (+Ara +Glc).

[e] ND, not determined.

we found another sequence within the *abnA* coding region (AAACAGTACGTACAAAA, at a position +831 relative to the transcription start site) similar to that of the AraR consensus operator (see above). We constructed an *abnA'-lacZ* fusion bearing this element to determine its involvement in the regulation of *abnA* expression (Fig. 1). The transcriptional fusion was integrated in a single copy at the *amyE* locus of the wild-type and *araR*-null mutant backgrounds, and the resulting strains IQB448 and IQB449 (Table 1), respectively, were analyzed as described above. In the presence of arabinose and arabinan, strain IQB448 showed a twofold increase in the level of regulation by AraR relative to that of strain IQB410 (Table 3), indicating that this putative operator might contribute to the regulation of *abnA* expression at the transcriptional level.

Binding of AraR to the promoter region of *xsa* and *abnA* genes. The ability of AraR to bind to the promoter region of *xsa* and *abnA* genes was determined by quantitative DNase I footprinting with DNA fragments from the plasmids harboring the transcriptional fusions as targets (see Materials and Methods). Two AraR binding sites were detected by DNase I footprinting in the *xsa* promoter region (Fig. 6). In the *xsa* coding strand, AraR protects the regions between positions −72 and −52 (OR_{X1}) and between positions −32 and −11 (OR_{X2}); similar sequences are protected in the noncoding strand (Fig. 6). A pattern of DNase I-enhanced and -diminished cleavage was observed between OR_{X1} and OR_{X2} (Fig. 5 and 6) that resembled the DNase I footprintings of the *araABDLMNPQ-abfA* operon and *araE* (22). AraR binding to the two in-phase operators of the *xsa* metabolic operon and of the transport gene promoter regions thus seems to occur in similar ways, producing in both cases a distortion of the DNA helix. Binding of AraR to OR_{X1} and OR_{X2} was also inhibited by the presence of arabinose (Fig. 6), indicating that arabinose is the effector which modulates AraR binding to DNA. The K_{app} for each individual binding site was determined as the repressor concentration at which half-maximal site occupancy was observed (Fig. 6). Although these values were calculated for a single experiment, the relative affinity of AraR to OR_{X1} and OR_{X2} is comparable to that observed for the AraR binding sites in the promoter regions of the metabolic operon and the *araE* gene (22). Binding of AraR to the putative OR_{B1} operator identified by sequence analysis within the *abnA* promoter was not detected in the same range of protein concentrations used for the *xsa* promoter (data not shown).

To assess the functionality of the AraR operators in vivo, we introduced the same single-base-pair substitution in both OR_{X2} and the putative OR_{B1} (Fig. 5). This mutation in a highly conserved position of the AraR target sequence (22) was designed to prevent the binding of AraR to OR_{X2} in the *xsa* promoter and to OR_{B1} in the *abnA* promoter. The two mutant promoters were fused to the *lacZ* gene of *E. coli* and were analyzed in a *B. subtilis* wild-type background as described above. Both mutations resulted in a loss of regulation by AraR (Table 4). These results indicate that just one base pair change in one of the two operators (OR_{X1} and OR_{X2}) is

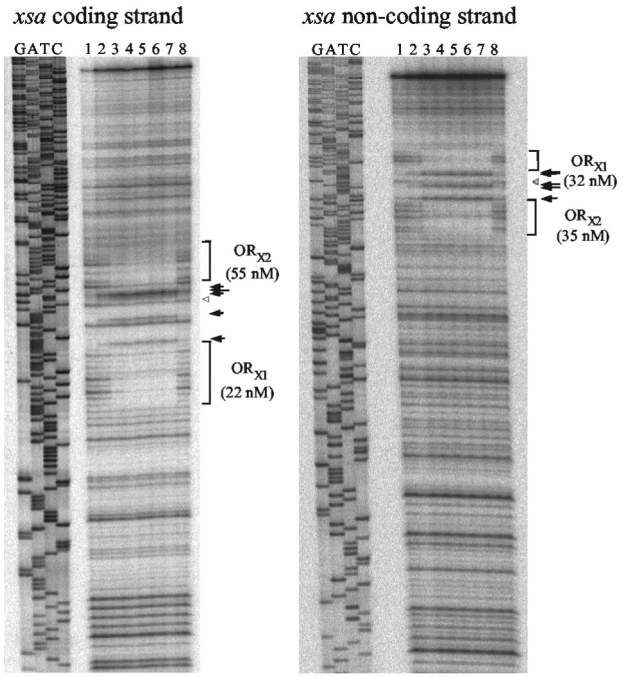

FIG. 6. DNase I protection experiments of the *xsa* promoter by the AraR protein. Each strand of a 339-bp DNA fragment carrying the *xsa* promoter region was end labeled with γ-^{32}P in separate experiments. AraR concentrations were calculated considering a pure dimeric protein. Lane 1, no protein; lane 2, 25 nM AraR; lane 3, 50 nM AraR; lane 4, 100 nM AraR; lane 5, 150 nM AraR; lane 6, 200 nM AraR; lane 7, 250 nM AraR; lane 8, 250 nM AraR plus 0.02% (wt/vol) L-arabinose. Protected regions, termed OR_{X1} and OR_{X2}, are indicated in the autoradiograms by brackets. The sites of enhanced (black arrows) and diminished (open triangles) DNase I cleavage outside of the protected regions are both indicated in the autoradiograms. The size of the arrow reflects the intensity of enhanced cleavage by DNase I. Total repressor concentration at which half-maximal site occupancy is achieved (a value that represents K_{app}, the apparent affinity of AraR to each site) is indicated within parentheses for each operator and was calculated from a single experiment.

sufficient to abolish repression and suggest cooperative binding to the two in-phase operators in the *xsa* promoter region. Furthermore, OR_{B1} is an active *cis*-acting element for the regulation of the *abnA* promoter.

DISCUSSION

In *B. subtilis*, the genes encoding hemicellulolytic enzymes are clustered with genes encoding enzymes that further catabolize these carbon sources (reference 35 and references therein). In this study, we analyzed the mechanisms that regulate the expression of three arabinan-degrading genes, *abfA*, *xsa*, and *abnA*, which are assembled with genes involved in arabinose catabolism (Fig. 1). The *abfA* and *xsa* genes most probably encode AFs (EC 3.2.1.55) belonging to the GH51 family (http://afmb.cnrs-mrs.fr/~cazy/CAZY). Although the exact subcellular localization of Xsa and AbfA is unknown, these enzymes are believed to be intracellular (1, 37). Nonetheless, AFs from *G. stearothermophilus* and *B. subtilis* were purified from supernatants of cultures at the end of the stationary phase (8, 13, 39). Based on primary amino acid sequence analysis, the *abnA* gene most likely encodes an ABN (EC 3.2.1.99) grouped in the GH43 family (http://afmb.cnrs-mrs.fr/~cazy/CAZY), which was shown to be extracellular (1). Here, we determined the function of the *abnA* gene by showing that an insertion-deletion mutation in this gene led to a loss of arabinanase activity (Fig. 2). However, the *abnA*-null mutant is still able to grow on minimal medium with arabinan as the sole carbon source. This result might be due to the activity of the *yxiA* gene product, a hypothetical arabinanase displaying 27% identity to AbnA (17).

During exponential growth, the expression from *abfA'-lacZ*, *xsA'-lacZ*, and *abnA'-lacZ* transcriptional fusions revealed that *abfA* and *xsa* are strongly induced by arabinose, whereas the induction of *abnA* is weak (Table 3). The levels of induction in response to arabinan are very similar for the three genes. However, the level of arabinan-mediated induction of *abfA* and *xsa* is considerably lower than that observed with arabinose, while the induction levels of *abnA* are similar in both cases. This result is most probably due to different kinetics of induction by arabinose among the promoters (see below). A disruption of the *araR* gene abolished the regulation of the three arabinan-degrading genes, suggesting that AraR plays a major role in the transcriptional control of these genes. Previously, it has been reported that the addition of arabinose to the medium causes an immediate cessation of growth in an *araR*-null mutant background, which is probably due to an intracellular increase of arabinose and consequently an increase of the

TABLE 4. Site-directed mutagenesis of the *xsa* and *abnA* promoters

Promoter fusion and strain (base substitution)	β-Galactosidase activity (Miller units)[a]			Repression factor[b]	
	−Ara	+Ara	+Arab	Ara	Arab
xsa'-lacZ					
IQB405 (wild type)	7.5 ± 0.2	177.3 ± 3.9	21.8 ± 0.7	23.7	2.9
IQB465 (OR_{X2}-27 G→T)	728.6 ± 67.6	580.3 ± 49.5	740.1 ± 102.1	0.8	1.0
abnA'-lacZ					
IQB410 (wild type)	3.2 ± 0.7	10.0 ± 0.8	15.2 ± 2.1	3.1	4.7
IQB464 (OR_{B1}-38 G→T)	63.7 ± 5.3	27.1 ± 3.3	73.2 ± 3.6	0.4	1.1

[a] The strains containing different promoter-*lacZ* fusions were grown on C minimal medium supplemented with casein hydrolysate in the absence of sugar (−Ara), in the presence of arabinose (+Ara), or in the presence of arabinan (+Arab). Samples were analyzed 2 h (t_2) after the addition of sugars. The levels of accumulated β-galactosidase activity represent the average of results from three independent experiments.

[b] AraR repression was calculated as the ratio of the level of expression (Miller units) obtained in the presence of arabinose (+Ara) or arabinan (+Arab) to the value determined in the absence of sugar (−Ara).

metabolic sugar phosphate intermediates that are toxic to the cell (31). This effect is not observed when arabinan is added to the cultures, indicating that the reduced levels of expression observed in the presence of this carbon source might be due to lower levels of intracellular arabinose during the exponential growth phase. Since the arabinan-mediated induction of the three promoters is strictly dependent on AraR, and arabinan itself is not the molecular inducer (data not shown), the observed arabinan induction should be the result of low levels of intracellular arabinose. As mentioned above, the arabinose-mediated induction of *xsa* and *abfA* promoters is higher than that of the *abnA* promoter, while the arabinan induction levels are identical in the three cases. Therefore, a likely explanation for these results is that a lower level of arabinose is enough to rapidly and fully induce the *abnA* promoter but not the *abfA* and *xsa* promoters. Taken together, these observations indicate that the AraR protein exerts a tight control of arabinose- and arabinan-inducible transcription of the *abfA* and *xsa* genes but that repression of the *abnA* gene is more flexible.

One of the mechanisms involved in the synthesis of many degradative enzymes in *B. subtilis* is mediated by transition phase regulation (7). Accordingly, when the transcriptional fusions are analyzed at early postexponential phase, the levels of expression of *abfA*, *xsa*, and *abnA* in response to arabinose and arabinan are higher than those observed during exponential growth (Table 3). This finding suggests that the arabinan-degrading genes are subject to temporal regulation. In agreement with our observations, by extracellular proteome analysis, Antelmann et al. (1) detected AbnA at higher levels during stationary phase. Interestingly, the temporal differences among the induced levels of expression that we noticed are more striking in the case of arabinan than for arabinose. This finding suggests that arabinan, or one of its degradation products, may play an important role in this process. However, it may also be due simply to a higher amount of intracellular free arabinose as a result of a higher level of AbnA during the stationary phase. The mechanisms underlying the temporal regulation of the arabinan-degrading genes are unknown, but studies are currently in progress to address this question. Nonetheless, the data presented here indicate that the arabinose repressor, AraR, also plays a crucial role in the control of *abfA*, *xsa*, and *abnA* expression during early postexponential phase. Additionally, glucose repression previously characterized for the *araABDLMNPQ-abfA* operon (11) seems to be mediated by a similar mechanism in the case of the *abnA* and *xsa* genes.

The DNase I footprinting analysis of the *xsa* promoter suggests that this gene should be regulated by AraR by a mechanism similar to that proposed for the *araABDLMNPQ-abfA* operon and the *araE* transport gene (22, 23). As in these two cases, the AraR binding sites are separated by approximately four turns of the DNA helix (41 bp), and a pattern of DNase I hypersensibility was observed in the interoperator region (Fig. 5 and 6). Furthermore, a single-base-pair change in one of the two operators (OR_{X1} and OR_{X2}) is sufficient to abolish AraR repression in vivo. By analogy, this finding suggests that the binding of AraR to the operators in the *xsa* promoter is cooperative, resulting in a distortion of the DNA helix that may be in the form of a small DNA loop. In contrast, noncooperative binding of AraR to one operator in the promoter region of the *abnA* gene, and possibly to a second operator located downstream within the *abnA* coding region (Tables 3 and 4), is less effective, as observed in the case of autoregulation of *araR* expression (22, 23). The fact that we could not detect in vitro binding of AraR to the promoter region of *abnA* might indicate a low affinity of the regulator to its operator site. However, one cannot exclude the possibility of additional *trans*-acting factors involved in the regulation of *abnA* expression which may contribute to AraR binding or which may directly control *abnA* expression. Together, these observations might explain the different mode of response to arabinose and arabinan of *abnA* expression compared to those of *xsa* and *abfA* during exponential growth (Table 3), which may reflect distinct physiological requirements. A tight control of the *xsa* and *abfA* genes ensures the expression of these intracellular enzymes solely when the arabinose inducer is present. On the other hand, a weak control of *abnA* allows for a low level of basal transcription of this extracellular enzyme.

Bacilli secrete a vast number of polysaccharide backbone-degrading enzymes, which produce relatively large oligosaccharide products. These units, disaccharides, trisaccharides, and oligosaccharides, enter the cell by specific transport systems and are further broken down by intracellular enzymes (4, 35). We have shown that in *B. subtilis*, arabinan is degraded by at least one extracellular hemicellulase, AbnA. The resulting products, arabinose, arabinobiose, arabinotriose, and arabinooligosaccharides, are transported by different systems. Arabinose enters the cell mainly through the AraE permease (33), and the uptake of arabinose oligomers most likely occurs via AraNPQ, an ABC-type transporter (32). These latter products might be further digested intracellularly by AbfA and Xsa. Interestingly, the AraE permease is also responsible for the transport of xylose and galactose into the cell (16). These three structurally different sugars, arabinose, xylose, and galactose, are frequently found associated in hemicelluloses. Furthermore, xylan- and xylose-utilizing genes are controlled by the XylR repressor, and no regulatory protein specifically controlling galactose utilization has been found (reference 35 and references therein). These observations suggest a coordinated expression, triggered by arabinose and mediated by AraR, of genes encoding enzymes responsible for extracellular degradation of arabinose-containing polysaccharides and transport systems and intracellular catabolism of arabinose, xylose, and galactose. Concerted regulation of the production of all pectin side-chain-cleaving enzymes in response to arabinose seems likely to occur in *Aspergillus* spp. (5). Thus, it will be interesting to know how this regulatory circuitry in response to arabinose is disseminated among hemicellulase-producing microorganisms.

ACKNOWLEDGMENTS

We thank Rita Teodoro and Susana S. Silva for constructing some plasmids and strains.

This work was supported by grant no. POCTI/AGR/36212/00 from Fundação para a Ciência e Tecnologia and FEDER.

REFERENCES

1. **Antelmann, H., H. Tjalsma, B. Voigt, S. Ohlmeier, S. Bron, J. M. van Dijl, and M. Hecker.** 2001. A proteomic view on genome-based signal peptide predictions. Genome Res. **11:**1484–1502.
2. **Beldman, G., H. A. Schols, S. M. Piston, M. J. F. Searl-van Leewen, and A. G. J. Vorangen.** 1997. Arabinans and arabinan degrading enzymes. Adv. Macromol. Carbohydr. Res. **1:**1–64.

3. **Debeche, T., N. Cummings, I. Connerton, P. Debeire, and M. J. O'Donohue.** 2000. Genetic and biochemical characterization of a highly thermostable α-L-arabinofuranosidase from *Thermobacillus xylanilyticus.* Appl. Environ. Microbiol. **66:**1734–1736.
4. **Deutscher, J., A. Galinier, and I. Martin-Verstraete.** 2002. Carbohydrate uptake and metabolism, p. 129–150. *In* A. L. Sonenshein, J. A. Hoch, and R. Losick (ed.), *Bacillus subtilis* and its closest relatives: from genes to cells. ASM Press, Washington, D.C.
5. **de Vries, R. P.** 2003. Regulation of *Aspergillus* genes encoding plant cell wall polysaccharide-degrading enzymes; relevance for industrial production. Appl. Microbiol. Biotechnol. **61:**10–20.
6. **de Vries, R. P., and J. Visser.** 2001. *Aspergillus* enzymes involved in degradation of plant cell wall polysaccharides. Microbiol. Mol. Biol. Rev. **65:**497–522.
7. **Ferrari, E., A. S. Jarnagin, and B. F. Schmidt.** 1993. Commercial production of extracellular enzymes, p. 917–937. *In* A. L. Sonenshein, J. A. Hoch, and R. Losick (ed.), *Bacillus subtilis* and other gram-positive bacteria: biochemistry, physiology, and molecular genetics. American Society for Microbiology, Washington, D.C.
8. **Gilead, S., and Y. Shoham.** 1995. Purification and characterization of an α-L-arabinofuranosidase from *Bacillus stearothermophilus* T-6. Appl. Environ. Microbiol. **61:**170–174.
9. **Hazlewood, G. P., and H. J. Gilbert.** 1998. Structure and function analysis of *Pseudomonas* plant cell wall hydrolases. Prog. Nucleic Acid Res. Mol. Biol. **61:**211–241.
10. **Helmann, J. D., and C. P. Moran, Jr.** 2002. RNA polymerase and sigma factors, p. 289–312. *In* A. L. Sonenshein, J. A. Hoch, and R. Losick (ed.), *Bacillus subtilis* and its closest relatives: from genes to cells. ASM Press, Washington, D.C.
11. **Inácio, J. M., C. Costa, and I. de Sá-Nogueira.** 2003. Distinct molecular mechanisms involved in carbon catabolite repression of the arabinose regulon in *Bacillus subtilis.* Microbiology **149:**2345–2355.
12. **Kaji, A., and T. Saheki.** 1975. Endo-arabanase from *Bacillus subtilis* F-11. Biochim. Biophys. Acta **410:**354–360.
13. **Kaneko, S., M. Sano, and I. Kusakabe.** 1994. Purification and some properties of α-L-arabinofuranosidase from *Bacillus subtilis* 3–6. Appl. Environ. Microbiol. **60:**3425–3428.
14. **Kim, J. H., and G. H. Chambliss.** 1997. Contacts between *Bacillus subtilis* catabolite regulatory protein CcpA and *amyO* target site. Nucleic Acids Res. **25:**3490–3496.
15. **Kosugi, A., K. Murashima, and R. H. Doi.** 2002. Characterization of two noncellulosomal subunits, ArfA and BgaA, from *Clostridium cellulovorans* that cooperate with the cellulosome in plant cell wall degradation. J. Bacteriol. **184:**6859–6865.
16. **Krispin, O., and R. Allmansberger.** 1998. The *Bacillus subtilis* AraE protein displays a broad substrate specificity for several different sugars. J. Bacteriol. **180:**3250–3252.
17. **Kunst, F., N. Ogasawara, I. Moszer, A. M. Albertini, G. Alloni, V. Azevedo, et al.** 1997. The complete genome sequence of the Gram-positive bacterium *Bacillus subtilis.* Nature **390:**249–256.
18. **Martin-Verstraete, I., J. Stülke, A. Klier, and G. Rapoport.** 1995. Two different mechanisms mediate catabolite repression of the *Bacillus subtilis* levanase operon. J. Bacteriol. **177:**6919–6927.
19. **McKie, V. A., G. W. Black, S. J. Millward-Sadler, G. P. Hazlewood, J. I. Laurie, and H. J. Gilbert.** 1997. Arabinanase A from *Pseudomonas fluorescens* subsp. *cellulosa* exhibits both an endo- and an exo- mode of action. Biochem. J. **323:**547–555.
20. **Miller, J. H.** 1972. Experiments in molecular genetics. Cold Spring Harbor Laboratory, Cold Spring Harbor, N.Y.
21. **Moran, C. P., Jr., N. Lang, S. F. J. LeGrice, G. Lee, M. Stephens, A. L. Sonenshein, J. Pero, and R. Losick.** 1982. Nucleotide sequences that signal the initiation of transcription in *Bacillus subtilis.* Mol. Gen. Genet. **186:**339–346.
22. **Mota, L. J., P. Tavares, and I. Sá-Nogueira.** 1999. Mode of action of AraR, the key regulator of L-arabinose metabolism in *Bacillus subtilis.* Mol. Microbiol. **33:**476–489.
23. **Mota, L. J., L. M. Sarmento, and I. de Sá-Nogueira.** 2001. Control of the arabinose regulon in *Bacillus subtilis* by AraR in vivo: crucial roles of operators, cooperativity, and DNA looping. J. Bacteriol. **183:**4190–4201.
24. **Pascal, M., F. Kunst, J. A. Lepesant, and R. Dedonder.** 1971. Characterization of two sucrase activities in *Bacillus subtilis* Marburg. Biochimie **53:**1059–1066.
25. **Perego, M.** 1993. Integrational vectors for genetic manipulation in *Bacillus subtilis*, p. 615–624. *In* A. L. Sonenshein, J. A. Hoch, and R. Losick (ed.), *Bacillus subtilis* and other gram-positive bacteria: biochemistry, physiology, and molecular genetics. American Society for Microbiology, Washington, D.C.
26. **Saha, B. C.** 2000. α-L-Arabinofuranosidases: biochemistry, molecular biology and application in biotechnology. Biotechnol. Adv. **18:**403–423.
27. **Saha, B. C.** 2003. Hemicellulose bioconversion. J. Ind. Microbiol. Biotechnol. **5:**279–291.
28. **Sakamoto, T., M. Yamada, H. Kawasaki, and T. Sakai.** 1997. Molecular cloning and nucleotide sequence of an endo-1,5-α-L-arabinase gene from *Bacillus subtilis.* Eur. J. Biochem. **245:**708–714.
29. **Sambrook, J., E. F. Fritsch, and T. Maniatis.** 1989. Molecular cloning: a laboratory manual, 2nd ed. Cold Spring Harbor Laboratory, Cold Spring Harbor, N.Y.
30. **Sá-Nogueira, I., and H. de Lencastre.** 1989. Cloning and characterization of *araA*, *araB*, and *araD*, the structural genes for L-arabinose utilization in *Bacillus subtilis.* J. Bacteriol. **171:**4088–4091.
31. **Sá-Nogueira, I., and L. J. Mota.** 1997. Negative regulation of L-arabinose metabolism in *Bacillus subtilis*: characterization of the *araR* (*araC*) gene. J. Bacteriol. **179:**1598–1608.
32. **Sá-Nogueira, I., T. V. Nogueira, S. Soares, and H. Lencastre.** 1997. The L-arabinose (*ara*) operon of *Bacillus subtilis*: nucleotide sequence, genetic organization and expression. Microbiology **143:**957–969.
33. **Sá-Nogueira, I., and S. S. Ramos.** 1997. Cloning, functional analysis, and transcriptional regulation of the *Bacillus subtilis araE* gene involved in L-arabinose utilization. J. Bacteriol. **179:**7705–7711.
34. **Shallom, D., and Y. Shoham.** 2003. Microbial hemicellulases. Curr. Opin. Microbiol. **3:**219–228.
35. **Stülke, J., and W. Hillen.** 2000. Regulation of carbon catabolism in *Bacillus* species. Annu. Rev. Microbiol. **54:**849–880.
36. **Takao, M., A. Yamaguchi, K. Yoshikawa, T. Terashita, and T. Sakai.** 2002. Molecular cloning of the gene encoding thermostable endo-1,5-alpha-L-arabinase of *Bacillus thermodenitrificans* TS-3 and its expression in *Bacillus subtilis.* Biosci. Biotechnol. Biochem. **66:**430–433.
37. **Tjalsma, H., A. Bolhuis, J. D. Jongbloed, S. Bron, and J. M. van Dijl.** 2000. Signal peptide-dependent protein transport in *Bacillus subtilis*: a genome-based survey of the secretome. Microbiol. Mol. Biol. Rev. **64:**515–547.
38. **Weickert, M. J., and G. H. Chambliss.** 1990. Site-directed mutagenesis of a catabolic repression operator sequence in *Bacillus subtilis.* Proc. Natl. Acad. Sci. USA **87:**6238–6242.
39. **Weinstein, L., and P. Albersheim.** 1979. Structure of plant cell walls. IX. Purification and partial purification of a wall-degrading endoarabanase and an arabinosidase from *Bacillus subtilis.* Plant Physiol. **63:**425–432.
40. **Wipat, A., N. Carter, S. C. Brignell, B. J. Guy, K. Piper, J. Sanders, P. T. Emmerson, and C. R. Harwood.** 1996. The *dnaB-pheA* (256 degrees-240 degrees) region of the *Bacillus subtilis* chromosome containing genes responsible for stress responses, the utilization of plant cell walls and primary metabolism. Microbiology **142:**3067–3078.
41. **Zalieckas, J. M., L. V. Wray, Jr., and S. H. Fisher.** 1998. Expression of the *Bacillus subtilis acsA* gene: position and sequence context affect *cre*-mediated carbon catabolite repression. J. Bacteriol. **180:**6649–6654.
42. **Zverlov, V. V., W. Liebl, M. Bachleitner, and W. H. Schwarz.** 1998. Nucleotide sequence of *arfB* of *Clostridium stercorarium*, and prediction of catalytic residues of α-L-arabinofuranosidases based on local similarity with several families of glycosyl hydrolases. FEMS Microbiol. Lett. **164:**337–343.